



HAL
open science

Characteristics of strain-induced crystallization in natural rubber during fatigue testing: in situ wide-angle x-ray diffraction measurements using synchrotron radiation

Stéphanie Beurrot-Borgarino, Bertrand Huneau, Erwan Verron, Dominique Thiaudière, Cristian Mocuta, A. Zozulya

► To cite this version:

Stéphanie Beurrot-Borgarino, Bertrand Huneau, Erwan Verron, Dominique Thiaudière, Cristian Mocuta, et al.. Characteristics of strain-induced crystallization in natural rubber during fatigue testing: in situ wide-angle x-ray diffraction measurements using synchrotron radiation. *Rubber Chemistry and Technology*, 2014, 87 (1), pp.184-196. 10.5254/rct.13.86977 . hal-01010226

HAL Id: hal-01010226

<https://hal.science/hal-01010226>

Submitted on 27 Sep 2017

HAL is a multi-disciplinary open access archive for the deposit and dissemination of scientific research documents, whether they are published or not. The documents may come from teaching and research institutions in France or abroad, or from public or private research centers.

L'archive ouverte pluridisciplinaire **HAL**, est destinée au dépôt et à la diffusion de documents scientifiques de niveau recherche, publiés ou non, émanant des établissements d'enseignement et de recherche français ou étrangers, des laboratoires publics ou privés.

CHARACTERISTICS OF STRAIN-INDUCED CRYSTALLIZATION IN NATURAL RUBBER DURING FATIGUE TESTING: IN SITU WIDE-ANGLE X-RAY DIFFRACTION MEASUREMENTS USING SYNCHROTRON RADIATION

S. BEURROT-BORGARINO,¹ B. HUNEAU,^{1,*} E. VERRON,¹ D. THIAUDIÈRE,² C. MOCUTA,² A. ZOZULYA²

¹ECOLE CENTRALE NANTES, INSTITUT DE RECHERCHE EN GÉNIE CIVIL ET MÉCANIQUE (GEM), UMR CNRS 6183,
BP 92101, 44321 NANTES CEDEX 3, FRANCE

²SYNCHROTRON SOLEIL, 91192 GIF-SUR-YVETTE, FRANCE

ABSTRACT

Strain-induced crystallization of carbon black-filled natural rubber is investigated by wide-angle X-ray diffraction (WAXD) during in situ fatigue tests using synchrotron radiation. Thanks to an original experimental method, we measure the evolution with the number of cycles of: (i) the index of crystallinity, both (ii) size and (iii) orientation of the crystallites, and finally (iv) the lattice parameters. It is shown that when the minimum stretch ratio of the fatigue test is lower than the onset of melting of the crystallites, then the index of crystallinity and the size of the crystallites decrease, whereas they increase when the minimum stretch ratio is higher than the onset of melting. For all the fatigue tests, the misorientation of the crystallites slightly decreases and the lattice parameters remain constant with the number of cycles. [doi:10.5254/rct.13.86977]

INTRODUCTION

Natural rubber (NR; cis-1,4-polyisoprene) vulcanizates have the ability to crystallize under strain at room temperature. Strain-induced crystallization (SIC) of NR was discovered by Katz in 1925 with the help of X-ray diffraction.¹ This technique has since permitted researchers to obtain the crystallographic data of NR,^{2,3} to evidence the existence of stretch ratio thresholds for crystallization and melting of the crystallites,^{4,5} to relate SIC to the mechanical hysteresis of the stress-strain response,⁴⁻⁶ and to put into light the effect of fillers such as carbon black.⁷ For more details on the use of X-ray diffraction for the investigation of SIC in NR, the reader can refer to the recent review by Huneau.⁸

The great majority of studies on the SIC of NR focus on quasi-static uniaxial tensile and relaxation tests. Nevertheless, NR is often used in engineering applications for its great properties in fatigue such as long fatigue life, even at large strain.⁹⁻¹¹ The mechanical properties of NR in fatigue have been thoroughly studied,¹²⁻¹⁵ but studies on the evolution of SIC during fatigue testing of NR are very rare, even though it is often accepted that its remarkable macroscopic fatigue properties are closely related to SIC (see, for example, Saintier et al.¹⁶ for the effect of positive loading ratio). This lack of investigation is mainly due to the typical frequencies of fatigue tests (1 Hz or more), which are not compatible with the long time acquisition required by X-ray diffraction measurements (from a few seconds to an hour). However, Kawai¹⁷ succeeded in measuring SIC during fatigue by using a stroboscopic technique to accumulate the weak intensity of the diffracted beam over a large number of cycles. He studied only one set of loading conditions for which both minimum and maximum stretch ratios of cycles are 3.5 and 4.5, respectively. More recently, Rouvière et al.¹⁸ measured the evolution of crystallinity along fatigue life for different uniaxial loading conditions by performing interrupted fatigue tests. As their method requires an exposure time of 45 min for the acquisition of the X-ray diffractogram, it does not allow the separation of SIC induced by fatigue from SIC induced by constant stretching. In both studies, only the degree of crystallinity of NR is measured,

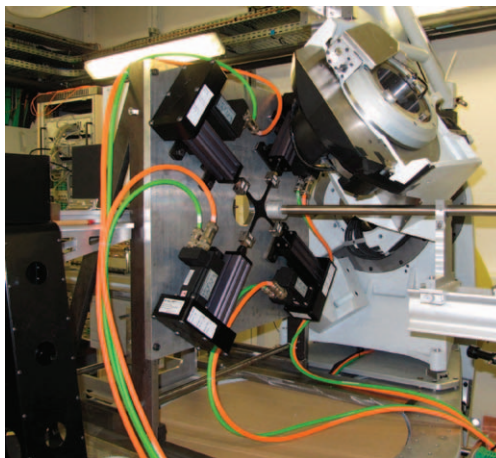


FIG. 1. — Fatigue-testing machine in DiffAbs beamline in synchrotron Soleil.

even though the X-ray diffraction technique allows for measuring more characteristics of the crystallized phase such as the size and orientation of the crystallites and the lattice parameters of the unit cells.

The aim of the present study is to measure the evolution of the different characteristics of the crystallized phase of NR during fatigue at different stretch ratios. For this purpose, an innovative experimental method that allows for the measurement of SIC in real time during a fatigue test was developed. In situ wide-angle X-ray diffraction (WAXD) measurements are performed with a very short exposure time thanks to synchrotron radiation.

EXPERIMENTAL PROCEDURE

INSTRUMENTATION

The synchrotron measurements have been carried out at the DiffAbs beamline in the French national synchrotron facility SOLEIL (proposal number 20100096). The wavelength used is 1.319 Å, and the beam size is 0.3 mm in diameter at half-maximum. The two-dimensional WAXD patterns are recorded by a MAR 345 CCD X-ray detector. The exposure time is 1 s, which is the minimum exposure time to record a workable scattering pattern. A PIN diode is used to measure the transmitted photons.

The experiments are conducted with the homemade stretching machine shown in Figure 1. It is composed of four electrical actuators, but only two opposite ones are used in this study, so that only uniaxial loading conditions are considered. Their movements are synchronized to keep the center of the specimen fixed during fatigue tests. Their loading capacity is ± 500 N, and their stroke is 75 mm each.

MATERIAL AND SAMPLES

The material is a carbon black-filled NR, cross-linked with 1.2 g of sulphur and 1.2 g of CBS accelerator for 100 g of rubber. It also contains 5 g of ZnO and 2 g of stearic acid and is filled with 50 g of N330 carbon black. The samples are classical flat dumbbell specimen with a 10 mm gauge length and a 2×4 mm² section.

Preliminary quasi-static tests are conducted beforehand to determine (1) the relation between the local stretch ratio λ at the center of the sample and the displacements of the grips and (2) the

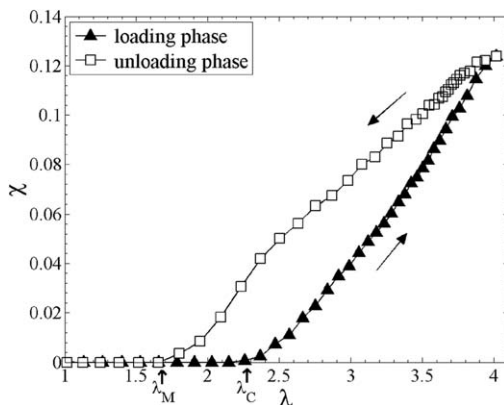


FIG. 2. — Evolution of the index of crystallinity during a quasi-static tensile test.

thresholds of crystallization λ_C and melting λ_M of the material at room temperature (similar to Trabelsi et al.⁵). Even if the experiments are not conducted at the same time, the same tensile machine is used, and the experimental conditions are set identical: first, a five-cycle accommodation of the sample is performed, then the sample is elongated to 100 mm at the speed of $0.012 \text{ mm}\cdot\text{s}^{-1}$, with the total duration of the corresponding cycle being about 2 h.

In the first experiment, the local stretch ratio λ is measured continuously as a function of the relative displacement of the grips outside the beamline with a motion analysis system (Tema motion[®]); in the second experiment, the local scattering pattern is recorded during 2 s every 98 s in the beamline and the index of crystallinity is obtained as a function of the relative displacement of the grips. Figure 2 is plotted with the two sets of data and presents the evolution of the index of crystallinity from $\lambda = 1$ to $\lambda = 4$ under quasi-static loading conditions (the order of magnitude of the strain rate $\dot{\lambda}$ is about 10^{-3} s^{-1}). It shows that the thresholds are $\lambda_C = 2.26$ on the loading path and $\lambda_M = 1.80$ on the unloading path for the material studied here.

PROCEDURES

To lower the residual stretch of the sample due to viscous and Mullins effects, all samples are recycled just before testing: 50 cycles at a higher strain level than during the tests.

The fatigue tests are conducted by prescribing constant displacements of the grips at each cycle. They are performed at conventional frequencies (i.e., about 1 Hz). As the minimum exposure time to record a diffraction pattern is 1 s (about the duration of a whole cycle), it is not possible to record diffraction patterns while the actuators are in motion. Therefore, to measure the evolution of SIC during fatigue testing, the tests are paused at maximum stretch ratio every 250 cycles to record a complete diffraction pattern. As the fatigue machine is triggered by the monitoring system of the X-ray beam, the duration of the pause is less than 1.5 s. The first scattering pattern is recorded at maximum strain of the first cycle of the test.

Four different fatigue tests are performed; Table I presents the minimum and maximum displacements of the grips d_{\min} and d_{\max} , the corresponding minimum and maximum stretch ratios λ_{\min} and λ_{\max} , and the loading frequency f .

SCATTERING PATTERN ANALYSIS

In this study, WAXD is used: the range of diffraction angles is $2\theta \in [8^\circ, 26.7^\circ]$. We use the (012) reflections of Cr_2O_3 powder placed on each side of a specimen to calibrate the diffraction angles 2θ

TABLE I
FATIGUE LOADING CONDITIONS

Test No.	d_{\min} , mm	d_{\max} , mm	λ_{\min}	λ_{\max}	f, Hz
1	0	20	1.00	2.90	2.5
2	4	33.2	1.44	3.66	0.8
3	9.3	33.2	1.98	3.66	1.0
4	25	45	3.18	4.02	1.5

(the lattice parameters of Cr_2O_3 are $a=4.9590 \text{ \AA}$ and $c=1.3596 \text{ \AA}$). Moreover, the well-established correction method of Ran et al.¹⁹ is adopted: an air-scattering pattern (without sample) is first collected and is used to correct the patterns, and the change in thickness of the sample under extension as well as the change of intensity of the incident photons are also considered (for the detailed description of the correction method, the reader can refer to the PhD thesis of Beurrot-Borgarino²⁰). An example of corrected diffraction pattern is given in Figure 3.

Once the corrections are performed, the intensity of photons diffracted by the isotropic phase of the material $I_{\text{iso}}(2\theta)$ is extracted from the diffraction patterns by considering the minimum intensity along the azimuthal angle β for each Bragg angle 2θ . Then, the intensity of photons diffracted by the anisotropic phase $I_{\text{ani}}(2\theta, \beta)$ is calculated as the difference between the total intensity of photons diffracted $I_{\text{total}}(2\theta, \beta)$ and $I_{\text{iso}}(2\theta)$. The spectra extracted from $I_{\text{ani}}(2\theta, \beta)$ and $I_{\text{iso}}(2\theta)$ are classically fitted by a series of Pearson functions.^{4,5,21,22} Different characteristics of the crystallized phase of NR are calculated from those quantities.

- An index of crystallinity χ :

$$\chi = \frac{I_{\text{cryst}}}{I_{\text{cryst}} + I_{\text{amorph}}} \quad (1)$$

where I_{cryst} is the integrated intensity of the (120) and (200) reflections measured on one spectrum ($2\theta, I_{\text{ani}}$), and I_{amorph} is the integrated intensity of the amorphous halo, assumed equal to the integrated intensity I_{iso} . The index χ is proportional to the degree of crystallinity of the material.

- The size l_{hkl} of the crystallites in the direction normal to the (hkl) diffraction planes, deduced from the Scherrer formula,²³

$$l_{hkl} = \frac{K\lambda}{FWHM_{2\theta}\cos\theta} \quad (2)$$

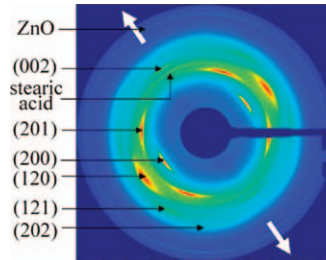


FIG. 3. — Example of diffraction pattern of crystallized NR in uniaxial tension. The white arrows show the tension direction. The Miller indices of the diffraction planes corresponding to the different reflections are indicated in the figure.

in which K is a scalar that depends on the shape of the crystallites (here we adopt 0.78 as proposed by Trabelsi et al.⁵), λ is the radiation wavelength, θ is the Bragg angle, and $FWHM_{2\theta}$ is the full width at half-maximum of the (hkl) reflection in 2θ .

- An index of the volume of the crystallites V_{cryst} deduced from the crystallites size in three different directions:

$$V_{cryst} = l_{200} \cdot l_{120} \cdot l_{201} \quad (3)$$

As the crystallites' shape is unknown, the actual volume of crystallites cannot be determined. Moreover, it is obvious that the product of mean sizes is not equal to the mean value of the product (i.e., the mean volume). Then, V_{cryst} is not proportional to the actual mean volume of the crystallites, but we consider it as a good qualitative indicator of the crystallites' volume.

- The misorientation ψ_{hkl} of the (hkl) diffraction planes in the crystallites (compared with their mean orientation) is simply given by half the full width at half-maximum ($FWHM_{\beta}$) of the peaks, measured on the azimuthal profiles of the reflection.
- Finally, the lattice parameters of the unit cell of the polyisoprene are calculated considering an orthorhombic crystal system, as determined by Immirzi et al.²⁴ and Rajkumar et al.²⁵ On the scattering patterns, 18 diffraction arcs due to six different diffraction planes are identified (see Figure 3). As only three lattice parameters (a , b , and c) must be calculated, each is the average of two values measured from reflections due to two different diffraction planes.

RESULTS AND DISCUSSION

As mentioned above, fatigue tests are performed by prescribing constant minimum and maximum displacements of the grips. As the material is cycled, Mullins and viscous effects lead to an increase of the sample length at zero stress; the local strain level reached at a given displacement then decreases with the number of cycles. This phenomenon is reduced by the accommodation of the material before fatigue testing, but it cannot be completely suppressed. Thus, all the results here are obtained for constant minimum and maximum displacements, which correspond to decreasing minimum and maximum strain levels. As shown in Table I, fatigue tests 1 and 2 are performed with minimum stretch ratios lower than λ_M . Moreover, even if the initial minimum stretch ratio in fatigue test 3 is slightly higher than λ_M , it becomes lower after only a few cycles, because the length of the sample at zero stress increases, as mentioned above. So, for these three tests, the same phenomenon takes place during each cycle: all the crystallites melt when the minimum displacement is reached, and new crystallites nucleate when the sample is stretched again. For fatigue test 4, the minimum stretch ratio achieved at each cycle decreases with the number of cycles as well, but it is always greatly larger than both the thresholds λ_M and λ_C . Therefore, some crystallites never melt, whereas some others melt at each cycle at low stretch ratios.

EVOLUTION OF χ DURING FATIGUE TESTS

The evolution of the index of crystallinity χ measured at maximum strain during fatigue tests is shown in Figure 4. As expected, the index of crystallinity depends on the stretch ratio: the larger the strain, the higher the crystallinity. Moreover, the index of crystallinity is equal during fatigue tests 2 and 3, which are performed at the same λ_{max} .

During the three fatigue tests with the lowest minimum and maximum strain levels (tests 1, 2, and 3; i.e., tests during which all the crystallites melt at each cycle), the index of crystallinity

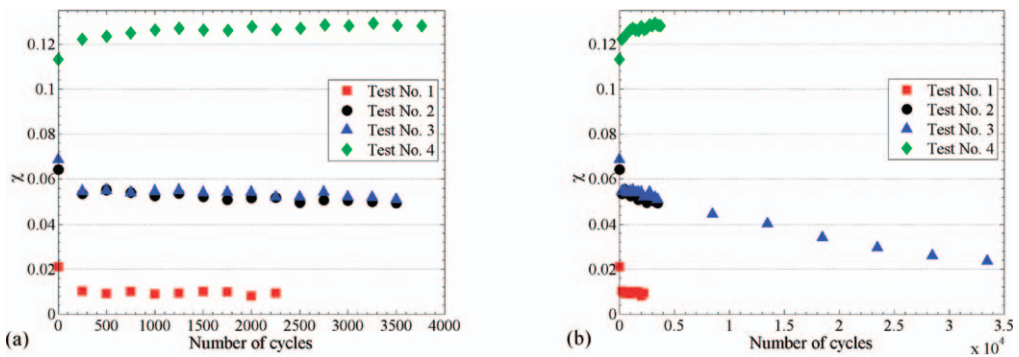


FIG. 4. — Evolution of the crystallinity index: (a) during the first 4000 cycles of fatigue tests 1 to 4; (b) during the first 35 000 cycles of test 3.

substantially decreased during the first 250 cycles: from 2.0% to 1.0% for test 1 and from about 6.5% to 5% for tests 2 and 3. Then it continued to decrease at a lower but constant rate until the end of the tests. Note that the results shown in Figure 4a correspond to only the first 4000 cycles of the fatigue tests, but test 3 has been performed during 35 000 cycles, as shown in Figure 4b, and χ is revealed to decrease at a constant rate during the whole test, down to about $\chi = 2.0\%$ in comparison with $\chi = 6.5\%$ at the beginning of the test.

During fatigue test 4, for which the minimum stretch ratio is higher than λ_C and λ_M , the evolution of the index of crystallinity differs: χ increases during the first 4000 cycles from 11.5% to 12.5%. This result is in agreement with those of Kawai¹⁷ obtained during a fatigue test with $\lambda_{\min} = 3.5$ and $\lambda_{\max} = 4.5$.

This aspect of the study has been thoroughly examined in ref. 26 and has led to the proposal of a scenario to explain the evolution of crystallinity under fatigue loading conditions. It will not be further analyzed in the present paper.

SIZE AND VOLUME OF THE CRYSTALLITES

Before examining the results, two preliminary remarks must be made.

First, the data of fatigue test 1 are not considered because the degree of crystallinity during this test is too small to allow good measurements on the diffraction arcs in the scattering patterns.

Second, as only a unique experiment has been conducted for each loading condition, no statistical uncertainty can be calculated. Moreover, the noise of raw WAXD data renders difficult an accurate determination of the Bragg angle θ and of the width of the diffraction peaks $FWHM_{2\theta}$; consequently, both crystallite size and index of the volume given by Eqs. 2 and 3 are subjected to uncertainty difficult to evaluate. Thus, only significant increases and decreases of the quantities will be considered and discussed.

Figures 5 and 6 show the evolution of the size of the crystallites during the first 4000 cycles of fatigue tests 2 and 3 and fatigue test 4, respectively. Only the size in the directions normal to the diffraction planes (120), (121), (200), and (201) are shown; the reflections (002) and (202) are too weak to be accurately measured. The size of the crystallites is very close for the three tests, even though λ_{\max} varies: $l_{120} \approx 50 \text{ \AA}$, $l_{121} \approx 45 \text{ \AA}$, $l_{200} \approx 125 \text{ \AA}$, and $l_{201} \approx 115 \text{ \AA}$. This result is consistent with the results of Poompradub et al.²⁷ and Trabelsi et al.⁷ for carbon black-filled NR. Moreover, the sizes measured here are very close to the sizes obtained during a high strain rate cycle for the same material at about $\dot{\lambda} = 6.4 \text{ s}^{-1}$.²⁰

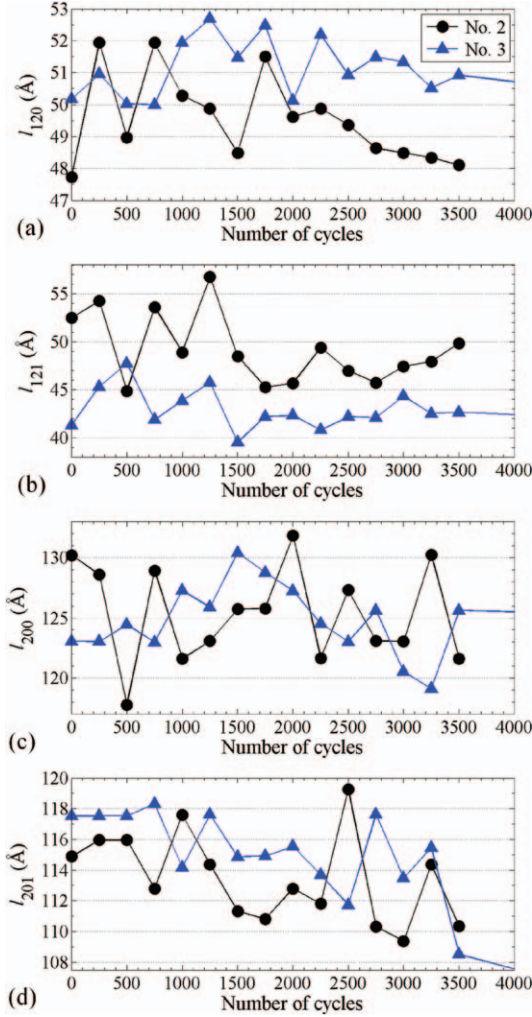


FIG. 5. — Evolution of the size of the crystallites during fatigue tests 2 and 3 in the directions normal to the diffraction planes (120), (121), (200), and (201).

During fatigue tests 2 and 3, the size of the crystallites slightly decreased, of a few percent during the first 4000 cycles (see Figure 5b,d). On the contrary, during fatigue test 4, the size of the crystallites increased in the four directions of about 8% (see Figure 6). The rate of increase is higher at the beginning of the test (during the first 250 cycles) than during the rest of the test.

The evolution of the index of the volume of crystallites during the three fatigue tests is shown in Figure 7; Figures 7a and b show the evolution during the first 4000 cycles and the first 13 500 cycles of tests 2 and 3, respectively, and Figure 7c shows the evolution during the first 4000 cycles of test 4. Obviously, the volume follows the same trend as the dimensions of the crystallites. On one hand, during tests 2 and 3, which are performed with λ_{\min} lower than the threshold of melting λ_M , the volume of the crystallites decreases with the number of cycles. This decrease may explain the decrease of χ observed in Figure 4, but its origin is still unexplained. Most probably, this decrease is not due to the decrease of λ_{\max} with the number of cycles during the fatigue tests; indeed, during a quasi-static test, the volume of the crystallites decreases when the stretch ratio increases.²⁰

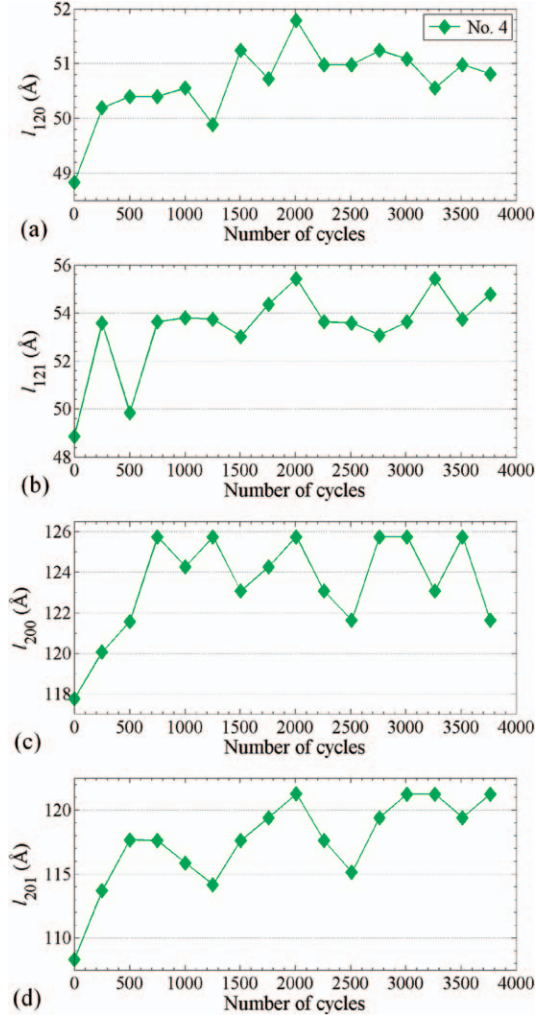


FIG. 6. — Evolution of the size of the crystallites during fatigue test 4 in the directions normal to the diffraction planes (120), (121), (200), and (201).

Furthermore, the decrease of the crystallites' size is surprising: as all crystallites melt at each cycle during the fatigue tests, it means that the new crystallites nucleate with a smaller size than the previous ones. On the other hand, during test 4, which is performed with λ_{\min} higher than the threshold of crystallization λ_C , the index of volume of the crystallites increases; it is consistent with the increase of χ observed in Figure 4. As previously, the origin of this evolution is unknown; in this case, it might be due to the decrease of λ_{\max} during the fatigue test, because it is established that during a quasi-static tensile test, V_{cryst} increases as λ decreases.²⁰

MISORIENTATION OF THE CRYSTALLITES

The evolution of the misorientation of the crystallites during fatigue tests is shown in Figure 8. Only the misorientation of the planes (120), (200), (201), and (002) are shown in Figures 8a to d, respectively; the measurements of the other diffraction planes are too noisy to be conclusive. The

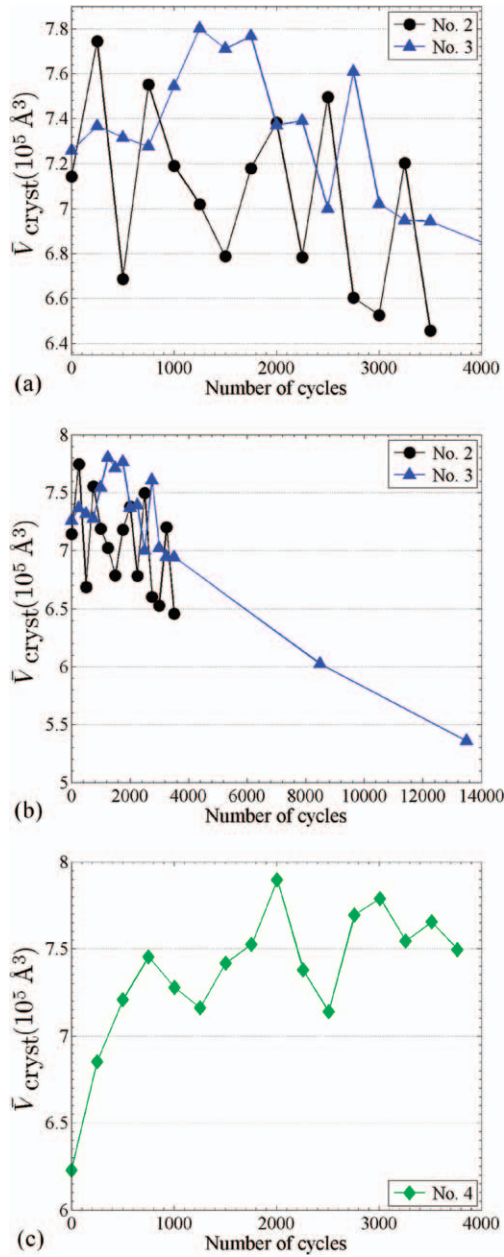


FIG. 7. — Evolution of the index of the volume of the crystallites (a) during the first 4000 cycles of fatigue tests 2 and 3; (b) during the first 13 500 cycles of fatigue test 3; and (c) during the first 4000 cycles of fatigue test 4.

misorientation of the crystallites ranges from 8° to 11.5° depending on the diffraction plane and the loading conditions. These values are similar to those measured by Poompradub et al.²⁷ and much smaller than those obtained by Trabelsi et al.⁷ during quasi-static uniaxial tensile tests of a carbon black-filled NR.

For the three fatigue tests, the misorientation of the crystallites decreases by about 5% to 15% during the first 250–500 cycles depending on the test and the diffraction plane considered, except

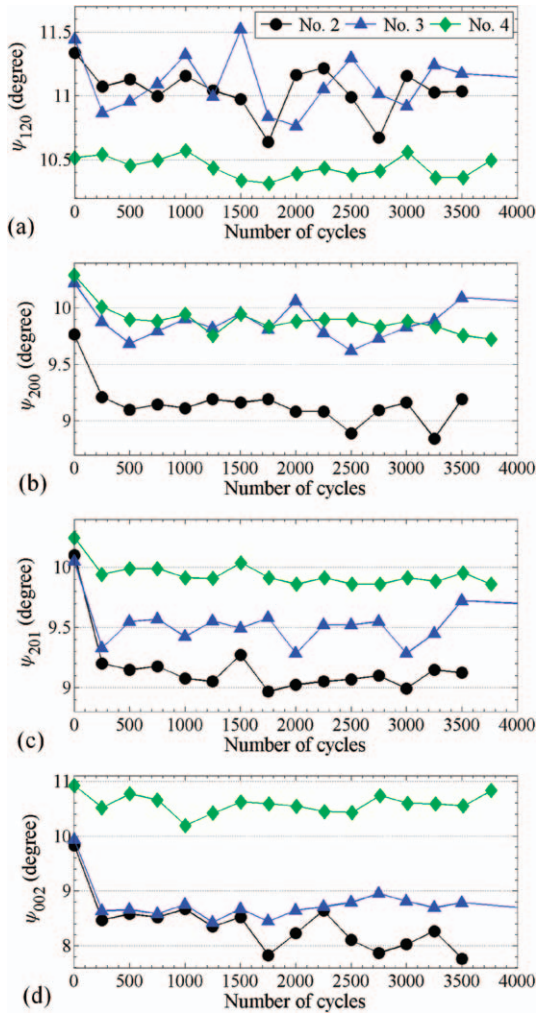


FIG. 8. — Evolution of the misorientation of the crystallites during the first 4000 cycles of fatigue tests 2 to 4.

for the (120) diffraction plane, for which misorientation remains almost constant. Then, during the rest of the fatigue tests, the misorientation does not change significantly. The initial decrease is smaller for fatigue test 4 than for the other tests. From a general point of view, the first few hundreds of cycles render the crystallites less misoriented for all the fatigue loading conditions.

For the (002) plane, our observations seem to be in agreement with those of Trabelsi et al.,⁷ who showed that ψ_{002} increases with λ during a quasi-static uniaxial tensile test: it is thus logical to measure a larger misorientation for fatigue test 4 than for tests 2 and 3 because the maximum stretch ratio is also larger (see Figure 8d). This unexpected increase of the misorientation of the c axis of the crystallites with the stretch ratio was confirmed by Beurrot-Borgarino,²⁰ who also showed that ψ_{120} decreases with λ during a quasi-static uniaxial tensile test between $\lambda = 3.5$ and $\lambda = 4$. This latter observation is thus consistent with Figure 8a, in which it is clearly seen that ψ_{120} is smaller for test 4 than for tests 2 and 3.

Figures 8b and c, in which ψ_{200} and ψ_{201} are plotted for the three different fatigue tests, are more difficult to discuss. They show that ψ_{200} and ψ_{201} depend on λ_{\min} , in particular for fatigue tests

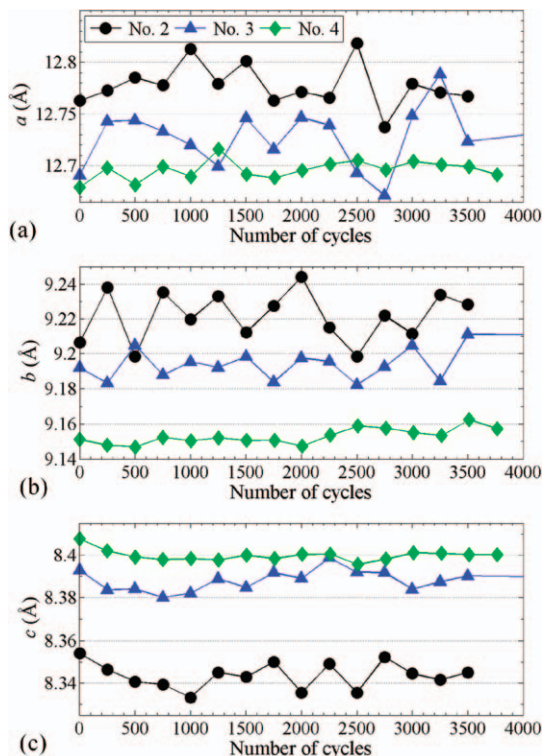


FIG. 9. — Evolution of the lattice parameters a , b , and c during fatigue tests 2 to 4.

2 and 3, for which $\lambda_{\min} < \lambda_M$ (i.e., when all the crystallites melt at each cycle). It would mean that the mechanical state of the amorphous phase when the minimum stretch ratio is reached has an influence on the orientation of the crystallites nucleated subsequently.

LATTICE PARAMETERS

Figure 9 shows the evolution of the lattice parameters a , b , and c during the first 4000 cycles of fatigue tests; beyond 4000 cycles for fatigue test 3, the crystallinity is too small to allow accurate measurements of the lattice parameters. Considering the three tests, the values of the lattice parameters are $12.67 \text{ \AA} < a < 12.80 \text{ \AA}$, $9.14 \text{ \AA} < b < 9.24 \text{ \AA}$, and $8.33 \text{ \AA} < c < 8.41 \text{ \AA}$. Note that these values vary by about 1% between the different tests. These values are similar to those obtained by Poompradub et al.²⁷ during a quasi-static uniaxial tensile test on a carbon black-filled NR.

Moreover, these authors and others show that under static loading conditions, a and b decrease and c increases with λ ; that is, the unit cell is more elongated in the tension direction and more contracted in the transverse directions.^{27–29} Consequently, it is relevant to observe that for test 4, which is performed at the highest λ_{\max} , a and b are smaller and c is higher than for tests 2 and 3. However, the lattice parameters differ highly between tests 2 and 3, whereas they are performed at the same λ_{\max} ; during test 2, which is performed at the lowest λ_{\min} , a and b are higher and c is lower than during test 3. This result is surprising considering that at each cycle during tests 2 and 3, all the crystallites melt and new ones nucleate when the material reaches λ_C . Once again, it would mean that the mechanical state of the amorphous phase at λ_{\min} has an influence on the subsequent crystallization that occurs at each cycle when λ reaches again λ_C .

CONCLUSION

To close this paper, we summarize the evolution of the different parameters of crystallization during fatigue tests performed at constant minimum and maximum displacements of the grips at each cycle:

- Crystallinity decreases with the number of cycles when $\lambda_{\min} < \lambda_M$ (i.e., when all the crystallites melt at each cycle). When $\lambda_{\min} > \lambda_M$ (i.e., when some of the crystallites never melt), the crystallinity increases with the number of cycles. Similarly to classical quasi-static tests, the crystallinity increases with λ_{\max} ; moreover, it does not depend on λ_{\min} when $\lambda_{\min} < \lambda_M$.
- The volume of the crystallites decreases with the number of cycles when $\lambda_{\min} < \lambda_M$, whereas it increases when $\lambda_{\min} > \lambda_M$. It can explain the decrease or the increase of the crystallinity mentioned above. Despite these changes during a fatigue test, the size of the crystallites does not depend significantly on λ_{\min} and λ_{\max} .
- For all fatigue loading conditions, the misorientation of the crystallites decreases during the first 250 or 500 cycles and is constant or slightly decreases through the rest of the fatigue test. This decrease is smaller when $\lambda_{\min} > \lambda_M$. Furthermore, the misorientation depends on both λ_{\min} and λ_{\max} .
- Experimental data do not exhibit any evolution of the lattice parameters with the number of cycles. However, a , b , and c depend on both λ_{\min} and λ_{\max} , even when all the crystallites melt at each cycle. For the highest value of λ_{\max} , the unit cell is logically more elongated in the tensile direction and retracted in the transverse directions.

To close this paper, one can note that the dependence of both crystallites' misorientation and lattice parameters with λ_{\min} suggests an influence of the mechanical state of the amorphous phase on strain-induced crystallization. This possible influence was not investigated in the present study and should be considered in further works.

REFERENCES

- ¹J. R. Katz, *Naturwissenschaften* **13**, 410 (1925).
- ²C. W. Bunn, *Proc. R. Soc. London, Ser. A* **180**, 40 (1942).
- ³S. C. Nyburg, *Acta Crystallographica* **7**, 385 (1954).
- ⁴S. Toki, T. Fujimaki, and M. Okuyama, *Polymer* **41**, 5423 (2000).
- ⁵S. Trabelsi, P. A. Albouy, and J. Rault, *Macromolecules* **36**, 7624 (2003).
- ⁶G. L. Clark, R. L. Le Tourneau, and J. M. Ball, *RUBBER CHEM. TECHNOL.* **14**, 546 (1941).
- ⁷S. Trabelsi, P. A. Albouy, and J. Rault, *Macromolecules* **36**, 9093 (2003).
- ⁸B. Huneau, *RUBBER CHEM. TECHNOL.* **84**, 425 (2011).
- ⁹S. M. Cadwell, R. A. Merrill, C. M. Sloman, and F. L. Yost, *Ind. Eng. Chem.* **12**, 19 (1940).
- ¹⁰N. André, G. Cailletaud, and R. Piques, *Kautsch. Gummi Kunstst.* **52**, 120 (1999).
- ¹¹N. Saintier, G. Cailletaud, and R. Piques, *Int. J. Fatigue* **28**, 530 (2006).
- ¹²W. V. Mars and A. Fatemi, *Int. J. Fatigue* **24**, 949 (2002).
- ¹³K. Legorju-Jago and C. Bathias, *Int. J. Fatigue* **24**, 85 (2002).
- ¹⁴V. Le Saux, Y. Marco, S. Calloch, C. Doudard, and P. Charrier, *Int. J. Fatigue* **32**, 1582 (2010).
- ¹⁵J.-B. Le Cam, B. Huneau, and E. Verron, *Int. J. Fatigue* **52**, 82 (2013).
- ¹⁶N. Saintier, G. Cailletaud, and R. Piques, *Mat. Sci. Eng. A* **528**, 1078 (2011).
- ¹⁷H. Kawai, *Rheol. Acta* **14**, 27 (1975).

- ¹⁸J. Y. Rouvière, A. Bennani, D. Pachoutinsky, J. Besson, and S. Cantournet, “Influence of mechanical and fatigue loading on crystallization of carbon black-filled natural rubber” in *Constitutive Models for Rubber V*, A. Boukamel, L. Laiarinandrasana, S. Méo, and E. Verron, Eds., Taylor & Francis/Balkema, Leiden, the Netherlands, 2008, 323.
- ¹⁹S. Ran, D. Fang, X. Zong, B. S. Hsiao, B. Chu, and P. F. Cunniff, *Polymer* **42**, 1601 (2001).
- ²⁰S. Beurrot-Borgarino, “Strain-Induced Crystallization of Natural Rubber in Fatigue and Multiaxial Deformation,” Ph.D. Thesis, Ecole Centrale de Nantes, France, 2012.
- ²¹J.-M. Chenal, C. Gauthier, L. Chazeau, L. Guy, and Y. Bomal, *Polymer* **48**, 6893 (2007).
- ²²J. Rault, J. Marchal, P. Judeinstein, and P. A. Albouy, *Eur. Phys. J. E: Soft Matter Biol. Phys.* **21**, 243 (2006).
- ²³A. Guinier. “X-ray Diffraction,” W. H. Freeman & Co, San Francisco & London, 1963.
- ²⁴A. Immirzi, C. Tedesco, G. Monaco, and A. E. Tonelli, *Macromolecules* **38**, 1223 (2005).
- ²⁵G. Rajkumar, J. M. Squire, and S. Arnott, *Macromolecules* **39**, 7004 (2006).
- ²⁶S. Beurrot-Borgarino, B. Huneau, E. Verron, and P. Rublon, *Int J. Fatigue* **47**, 1 (2013).
- ²⁷S. Poompradub, M. Tosaka, S. Kohjiya, Y. Ikeda, S. Toki, I. Sics, and B. S. Hsiao, *J. Appl. Phys.* **97**, 103529 (2005).
- ²⁸M. Tosaka, S. Murakami, S. Poompradub, S. Kohjiya, Y. Ikeda, S. Toki, I. Sics, and B. S. Hsiao, *Macromolecules* **37**, 3299 (2004).
- ²⁹M. Tosaka, *Polym. J.* **39**, 1207 (2007).